Sea-salt Aerosol Fluxes from Breaking Waves and Bursting Bubbles: Microphysical, Optical and Spatial Evolution in a Natural Wind-Tunnel

Antony D. Clarke
Department of Oceanography
University of Hawaii
1000 Pope Rd.
Honolulu, HI 96822
phone: (808) 956-6215 fax: (808) 956-7112 email: tclarke@soest.hawaii.edu

Vladimir N. Kapustin
phone: (808) 956-7777 fax: (808) 956-7112 email: kapustin@soest.hawaii.edu

Jingchuan Zhou
phone: (808) 956-7777 fax: (808) 956-7112 email: jczhou@hawaii.edu

Award Number: N00014-04-1-0308
http://www.soest.hawaii.edu/HIGEAR/

LONG-TERM GOAL

Our long-term goal is to establish an improved understanding of the properties and factors that control the marine aerosol generation processes, their dependence on oceanic and environmental conditions and aerosol evolution in the marine boundary layer.

OBJECTIVES

Our main objective is to investigate marine aerosol physiochemical and optical properties including pseudo-Lagrangian studies of their production, source flux, mixing and evolution in the boundary layer and coastal regions. We will focus on three-dimensional variability of aerosol fields in response to surface generation processes and links to whitecap coverage including various dependencies on oceanic and environmental conditions. We will utilize the wide range of wind speeds and conditions present in a natural "wind tunnel" in Hawaii and our aerosol and optical instrumentation to determine the open-ocean size-resolved production flux of sea-salt under diverse conditions and its vertical evolution in the marine boundary layer.

APPROACH

Our ongoing studies have been focused upon measurements of sea-salt production from open-ocean breaking waves during wave and whitecap intensification over a 100km fetch present in the natural "wind tunnel" between the islands of Maui and Hawaii. We have deployed the aerosol instrumentation package aboard the Young Brother's tug that biweekly plies the route up the Alenuihaha channel. The package has been deployed in March of 2005 and operated continuously during spring-summer 2005 to generate a "climatological" data base on channel aerosol generation.

Report Documentation Page

Form Approved
OMB No. 0704-0188

1. REPORT DATE	2. REPORT TYPE	3. DATES COVERED
30 SEP 2005		**00-00-2005 to 00-00-2005**

4. TITLE AND SUBTITLE	5a. CONTRACT NUMBER
Sea-salt Aerosol Fluxes from Breaking Waves and Bursting Bubbles: Microphysical, Optical and Spatial Evolution in a Natural Wind-Tunnel	5b. GRANT NUMBER
	5c. PROGRAM ELEMENT NUMBER
6. AUTHOR(S)	5d. PROJECT NUMBER
	5e. TASK NUMBER
	5f. WORK UNIT NUMBER
7. PERFORMING ORGANIZATION NAME(S) AND ADDRESS(ES) **University of Hawaii,Department of Oceanography,1000 Pope Rd.,Honolulu,HI,96822**	8. PERFORMING ORGANIZATION REPORT NUMBER
9. SPONSORING/MONITORING AGENCY NAME(S) AND ADDRESS(ES)	10. SPONSOR/MONITOR'S ACRONYM(S)
	11. SPONSOR/MONITOR'S REPORT NUMBER(S)

12. DISTRIBUTION/AVAILABILITY STATEMENT
Approved for public release; distribution unlimited

13. SUPPLEMENTARY NOTES
code 1 only

14. ABSTRACT
Our long-term goal is to establish an improved understanding of the properties and factors that control the marine aerosol generation processes, their dependence on oceanic and environmental conditions and aerosol evolution in the marine boundary layer.

15. SUBJECT TERMS

16. SECURITY CLASSIFICATION OF:			17. LIMITATION OF ABSTRACT	18. NUMBER OF PAGES	19a. NAME OF RESPONSIBLE PERSON
a. REPORT	b. ABSTRACT	c. THIS PAGE			
unclassified	**unclassified**	**unclassified**	**Same as Report (SAR)**	**9**	

WORK COMPLETED (2004-2005)

We have assembled and tested the autonomous instrumentation package for the Young Brother's tug (**Figure 1)**. The package includes the tandem nephelometers that operate with and without impactor in order to determine total and submicron light scattering. It also includes unheated and heated (300°C) condensation nuclei (CN) counters in order to resolve variations in total CN and refractory CN associated with sea salt. The details of our aerosol instrumentation are discussed elsewhere [1,2]. A mini-FSSP with an aspirated flow at 15 ms^{-1} and APS provide the aerosol size distribution between 0.8 and 50μm. The CCD camera provides continuous whitecap coverage and a combined GPS, wind speed, inclinometer and flux gate compass provide wind direction and speed corrected for ship movement. Lower boundary layer structure and visibility has been characterized with Vaisala Ceilometer and Visibility Meter. Instrumentation operates unattended under computer (LabView) control.

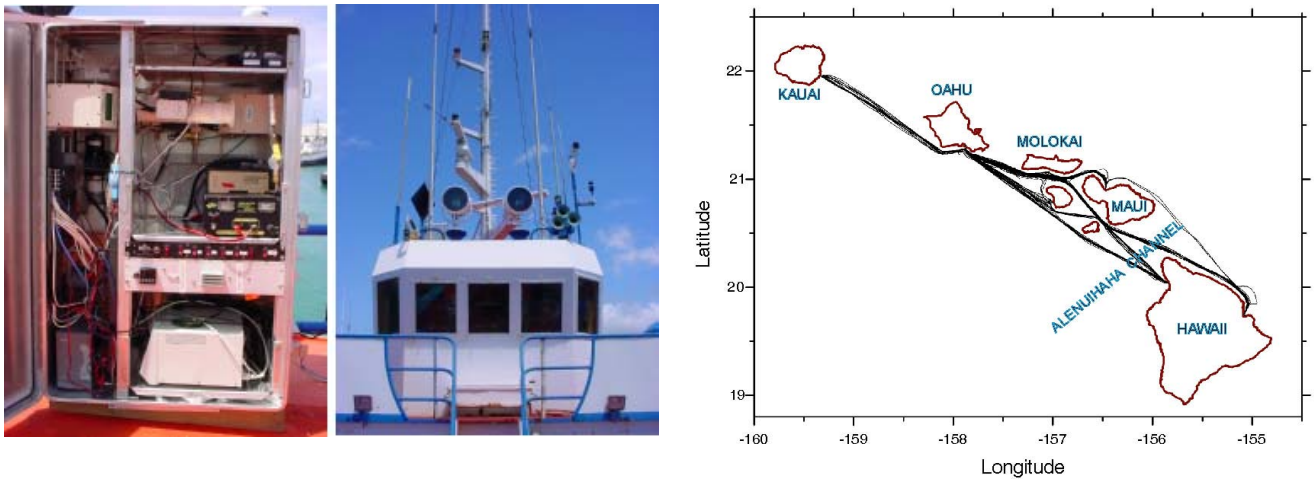

Figure 1. (left) Instrumentation package with total and submicrometer nephelometers, APS, Hot/cold CN, GPS, meteorological data and ceilometer (mini- lidar). (center) Instrument package is mounted atop the bridge of the tug. (right)Tugboat routs during 2005 aerosol measurements.

This package has been deployed in March of 2005 and operated continuously during spring-summer field season. We have collected a five-month duration aerosol data set including 54 Alenuihaha channel crossings (**Figure 1, right)**. We have demonstrated that, due to island mountain topography, the induced steady-state accelerated trade-wind flow in the Alenuihaha channel provides an ideal natural "wind-tunnel" for the study of sea-salt aerosol production, turbulent mixing, particle fluxes and related optical effects under real oceanic conditions.

RESULTS

The Alenuihaha channel is commonly aligned with the trade winds and provides about 100km of fetch. The winds are focused by mountains on Maui and the Big Island that can nearly double wind speeds over those of the open-ocean trade wind region, as seen in the MM5 model output for the Hawaiian Islands (**Figure 2**). This enhances the waves and sea-salt production [3,4].

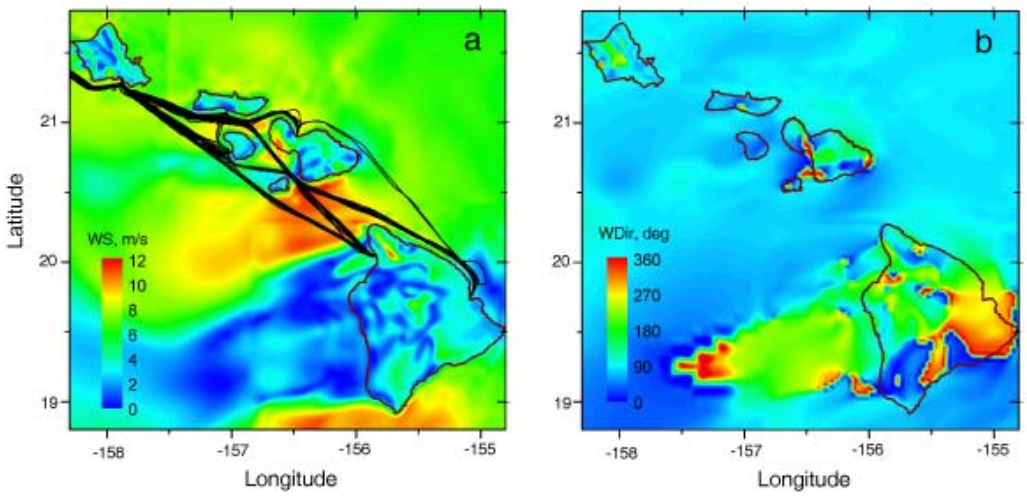

Figure 2. MM5 wind speed (a) and wind direction (b) around the Hawaiian Islands (color-coded) with tugboat route (black line) between Oahu and the Big Island. Note very enhanced winds in main Alenuihaha channel.

Tugboat routes within the Alenuihaha channel followed four branches (**Figure 3, right**), each with a distinct wind speed pattern (**Figure3, left**). Measured winds (**Figure 3,right**) are color coded along routes and reveal good agreement with typical MM5 winds (**Figure 2a**). Availability of MM5 winds will allow us to estimate the wind speed upstream the channel that we can relate to the background sea salt concentrations.

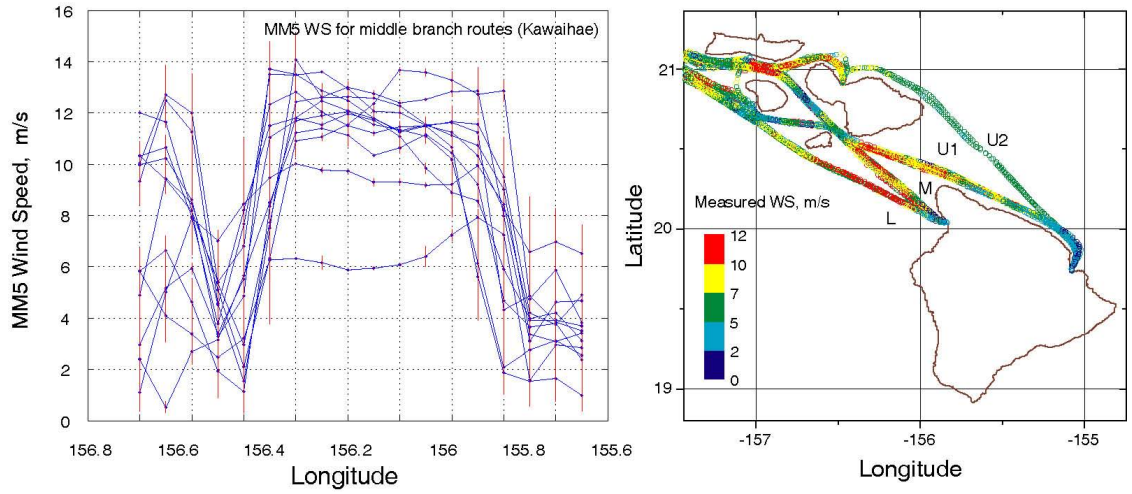

Figure 3. MM5 wind speed for middle branch routes in the channel (a) and tugboat routes color coded with wind speed (b) for lower (L), middle (M) and two upper (U1&U2) branches.

The wind speed enhancement and corresponding increase in aerosol concentration and light scattering are evident in our near-surface lidar data and light scattering data (**Figure 4**) taken from aboard ship along the transect line. Ceilometer lidar backscatter (red) for the near-surface 0-30m range compared with in-situ (blue) and "dry" (measured at RH~30%) total (black) and submicrometer (green)

nephelometer scattering data. During stable trade wind conditions supermicrometer (Dp > 1um) sea-salt dominates scattering and backscattering. The ratio of supermicrometer (Dp>1 um) to submicrometer (Dp<1 um) scattering (ScatRatio) has an average value of 2.5 and typically increases in the channel. This enhancement in supermicrometer scattering reflects increase of large sea-salt particle concentration and provides one of the possible explanations of the relative differences between ceilometer backscatter measured at wavelength of 0.905 um and in-situ nephelometer scattering measured at wavelength of 0.55 um.

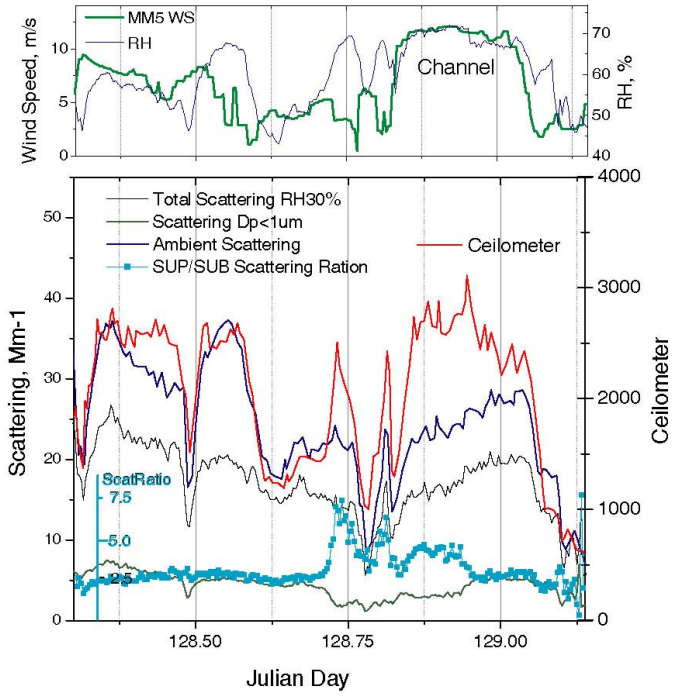

Figure 4. (top) MM5 winds along tugboat route showing the enhancement in channel. (bottom) Ceilometer lidar backscatter for the near-surface 0-30m range compared with in-situ (blue) and "dry" total (black) and submicrometer (green) scattering data. Supermicrometer sea-salt dominates scattering and backscattering data (ScatRatio, cyan).

As expected, the light scattering and other aerosol parameters measured within the channel are coupled to variations in wind speed. A scatterplot of the scattering at 30% RH for the entire field measurements period is shown in **Figure 5** and reveals a slope indicative of a local wind speed dependence but with a large spread of data points indicative of other processes influencing scattering, as found in our earlier studies over the Southern Ocean [4]. Because wind speeds were not equally distributed over the range of observed values we have used this data to calculate the mean and standard deviation of observed extinction for each interval of 1 ms^{-1} of wind speed.

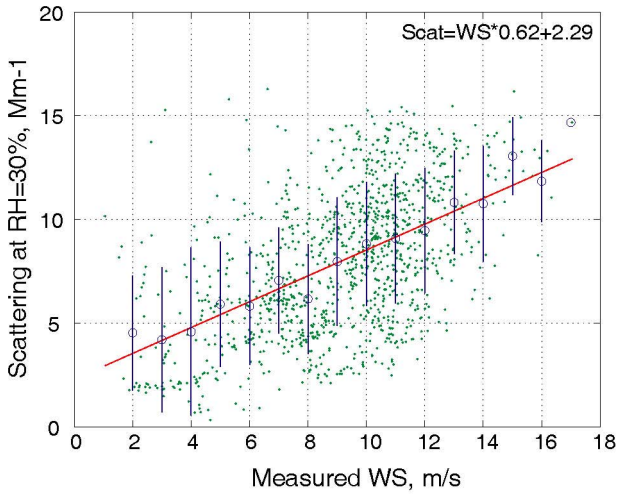

Figure 5. Relationship between average light scattering at 30% RH for binned wind speed (blue circles – mean values, blue bars –standard deviations) with green dots showing the raw data. Red line – linear regression of the light scattering data.

The result is a nearly linear dependence of scattering on wind speed between about 2 and 16 ms^{-1}. If we divide the scattering values by the nominal mass scattering efficiency of 1.2 m^2g^{-1} for dry sea-salt this figure also describes the optically effective mass dependence upon 10m wind speed, U_{10}. This is often written as $\ln (M/M_o) = a_M U_{10}$ where a_M describes the dependency. Here, the value of a_M from this bin averaged dependency is 0.13 and consistent with many reported values (Table 11, Lewis and Schwartz, 2004). However, these wind related enhancement in aerosol concentrations and scattering reveal more detailed structure when examined as individual cross-wind transects. **Figure 6a** shows lidar data up to 1,200m with 30m resolution for the day when clouds were also present. In **Figure 6b** we show the MODIS cloud field for that day with a red line indicating the route taken by the tug. The mean trade wind speed upwind the channel for this day was 11.9 m/s. Note that the clouds are aligned in "cloud streets" reflecting boundary layer rolls (to be discussed later). The clouds are also evident as high backscatter (red) in the **Figure 6a** lidar data. Note the fingerlike projections of high backscatter originating near the surface below clouds and the lower backscatter tongues (blue) projecting down between them. Some of this difference is related to rising air with higher relative humidity (RH) below cloud and tongues with lower RH (possible effect of entrained dry air) between them. However, near-surface dry coarse aerosol scattering (not shown) is also enhanced in the rising fingers indicating both sea-salt aerosol and RH are higher in these rising regions. Both enhanced sea-salt production under high wind and the relation to activated cloud droplets will be explored in this environment. In **Figures 6 c,d** we show similar data but for the day when clouds within the channel were infrequent but lidar data did show similar fingerlike organized structures. Note the large difference in column backscatter for the two images at wind speeds of 11.9 and 9.7 m s^{-1}. For a nominal cubic dependence of white cap coverage on wind speed [6] we would expect about doubling of white cap coverage (sea-salt production) for this wind speed increase. However, they point out that this relationship remains highly uncertain (Figures 36 and 37 in [6]). Quantifying such lidar features in terms of sea-salt production remains one of our planned objectives with future aircraft studies.

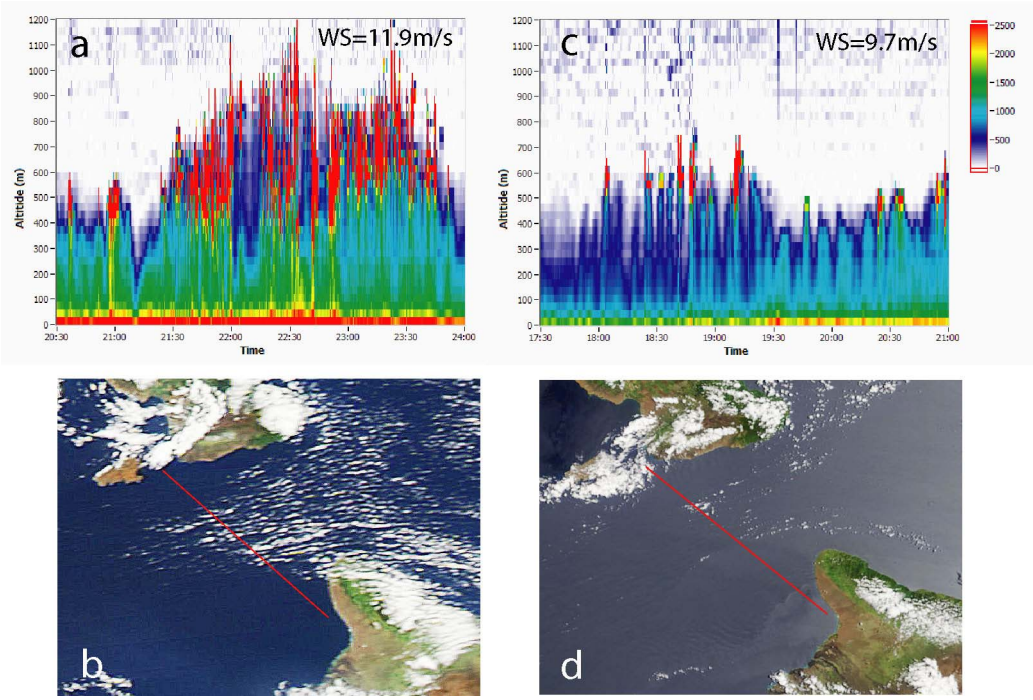

Figure 6. (top) Ceilometer lidar (905nm) imagery during crossing of Alenuihaha channel between Maui and the Big Island of Hawaii is sensitive to coarse sea-salt backscatter and reveals vertical fingers of enhanced backscatter below clouds (red). (bottom) Route for tug (orange) superimposed upon MODIS image revealing related "cloud streets" for same days.

The above aerosol features are linked to the dynamic features of near surface flow around the islands under trade wind conditions. These are illustrated in a figure taken from [5] and reproduced in **Figure 7a**. This figure exhibits the influence of the island topography on the trade wind flow and the huge down stream eddy that forms behind it. The influence of the volcano dominates the recirculated air in the southern half of the eddy (region 3) and enhanced sea-salt dominated the northern half of the eddy (region 2). In addition to these large scale features we note that smaller scale features such as cloud streets (**Figure 7b**) also influence the aerosol and optical structure in the boundary layer aerosol. These are evident in almost all flow regimes around the island including the cloud streets present in **Figure 6 b**. Our ONR tug results are finding that these boundary layer rolls or large organized eddies (LOE) are a common feature of the Hawaii environment and are evident in most of our data and also MODIS images. Even cloud free regions in satellite imagery include indications of these rolls organized along the wind in the channel as evident in the fingerlike structure generally observed in our lidar data (see **Figure 6 c,d)**.

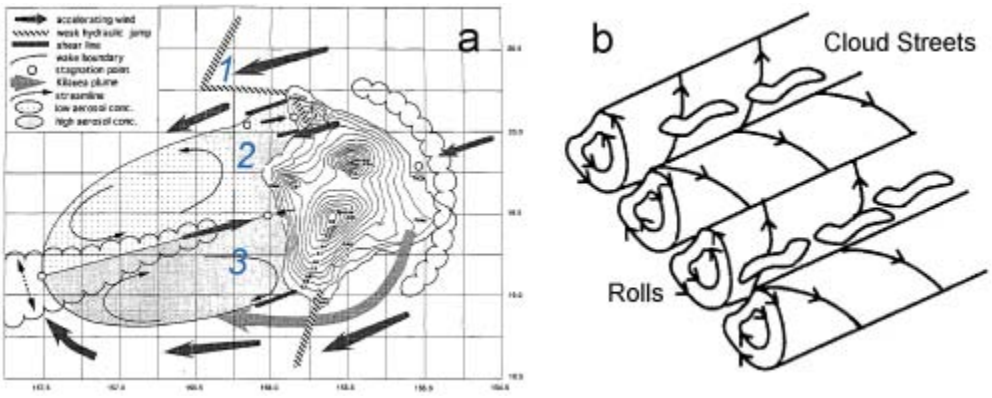

Figure 7. a) A conceptual picture of boundary layer flow around the Big Island. Region 1 is in the man channel flow, region 2 is light circulating winds with primarily seas-salt and region 3 is light recirculating winds with enhanced sulfate. b) Large organized eddies (LOE or rolls) with embedded cloud streets.

One issue we have also tried to pursue is obtaining open-ocean evidence for the new source function that includes sea-salt sizes down to 10nm, as we previously established for breaking waves [2]. This is much more difficult at sea where the impact of individual waves cannot be isolated and the instrumentation is more limited. Even so, our coastal observations demonstrated that breaking waves produced large numbers of small sea-salt (Dp< 100nm) identified as refractory condensation nuclei (CN) that were highly correlated with the few large ones that dominated the light scattering. **Figure 8** shows a similar high correlation of increased light scattering with increasing refractory CN measured under increasing wind in the open waters of the Alenuihaha Channel. Here about 30 refractory CN correspond to a change in scattering of about 4 Mm^{-1}. The coastal data measured only 10s after the breaking waves had a change in scattering of 16 Mm^{-1} for 30 refractory CN. This is to be expected at the open ocean will be much more aged and relatively depleted in coarse sizes that influence light scattering. Even so, this relation demonstrates that production of small sea-salt is also effective over the open ocean.

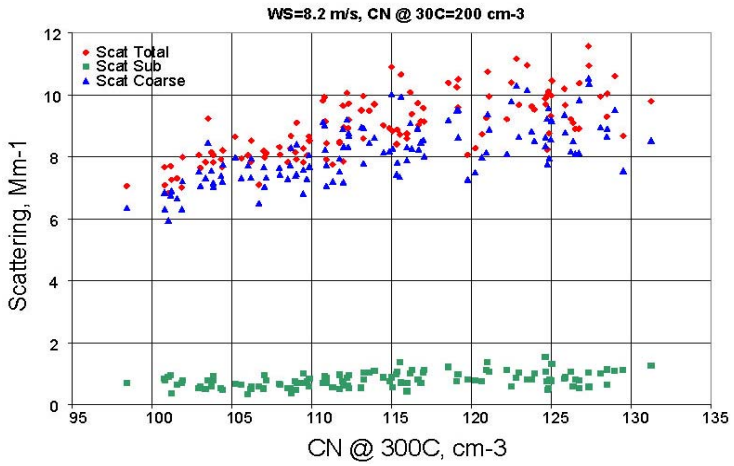

Figure 8. A plot of light scattering for total scattering (red) and submicron (green) showing dominance of coarse sea-salt and its relation to refractory CN at 300C.

Our plans for next year include the continued analysis of this data set and the integration of aircraft data collected in conjunction with the tug data. We will secure a new lidar for the aircraft and continue using the lidar on the tug as shown here to investigate the production of sea-salt by enhanced whitecap coverage and role of boundary layer rolls in processing this aerosol. We expect to scale back tug instrumentation to the lidar, visibility sensor, CN counter and met data as we transition to the aircraft data system.

REFERENCES

1. Clarke, A.D., Kapustin, Vladimir N. 2003a: The Shoreline Environment Aerosol Study (SEAS): A Context for Marine Aerosol Measurements Influenced by a Coastal Environment and Long-Range Transport. *Journal of Atmospheric and Oceanic Technology*: Vol. 20, No. 10, pp. 1351–1361.

2. Clarke, A.D, Kapustin, V., Howell, S., Moore, K., Lienert, B., Masonis, S., Anderson, T., Covert, D. 2003b: Sea-Salt Size Distributions from Breaking Waves: Implications for Marine Aerosol Production and Optical Extinction Measurements during SEAS. *Journal of Atmospheric and Oceanic Technology*: Vol. 20, No. 10, pp. 1362–1374.

3. Clarke, A.D., 2004: Marine Aerosol Sources: Bursting Bubbles, Entrainment and Cloud Condensation Nuclei. Submitted to GRL.

4. Shinozuka, Y., A.D. Clarke, S.G. Howell, V.N. Kapustin, and B.J. Huebert (2004), Sea-salt vertical profiles over the Southern and tropical Pacific oceans: Microphysics, optical properties, spatial variability, and variations with wind speed, *J. Geophys. Res.*, *109*, (D24), 1-18, D24201, doi:10.1029/2004JD004975.

5. Smith, R.B., and V. Grubisic (1993), Aerial Observations of Hawaii Wake, *Journal of the Atmospheric Sciences*, *50*, (22), 3728-3750.

6. Lewis, E.R., and S.E. Schwartz (2004), *Sea Salt Aerosol Production: Mechanisms, Methods, Measurements and Models*, AGU Monograph Series 152, Washington. D.C., 2004.